The spectral nature of solar phototurbulence

March 18, 2020, Revision: 1.22

1 Preliminaries

In the Sun, the radiative diffusivity is at least four orders of magnitude larger than the viscosity. This means that the Prandtl number, i.e., the ratio of kinematic viscosity to thermal or radiative diffusivity is always below 10^{-4}. One would therefore expect the temperature field to be always much smoother than the velocity field. However, on small length scales—comparable to the viscous diffusive cutoff or Kolmogorov scale—the radiative diffusion approximation breaks down. The gas experiences Newtonian cooling rather than photon diffusion. Such cooling is independent of the scale of the temperature structures and is thus no longer increasing toward smaller scales, as in Fickian diffusion. This means that our intuition about a smooth temperature field owing to a low Prandtl number may need to be reconsidered. Here we explore some of the consequences of this idea using simple numerical experiments.

In thinking about a minimalistic numerical experiment, it is useful to remember that turbulence is constantly dissipating energy through viscosity—even if the viscosity is extremely small. This source of heating is always present and can be significant in high Reynolds number turbulence. This heating may already be sufficient for a simple numerical experiment. Thus, we consider turbulence, here sustained by volume forcing in a small domain within the Sun. The effects of gravity and surface cooling, which can give rise convection, will be omitted, so we restrict ourselves to isotropic turbulence using triply-periodic boundary conditions.

In the Sun, the photon mean-free path is given by $\ell_\gamma = (\kappa\rho)^{-1}$, where κ is the specific opacity and ρ is the density. We find it convenient to work here instead with the wavenumber or inverse length scale and therefore refer to the critical photon wavenumber $k_\gamma = \kappa\rho$, above which radiation works predominantly through Newtonian heat exchange. The Kolmogorov wavenumber depends on the viscosity ν and the mean rate of energy dissipation ϵ and is given by $k_\nu = (\epsilon/\nu^3)^{1/4}$. This is the largest wavenumber of the inertial range, beyond which the spectral kinetic energy begins to fall off exponentially. Analogously, we can define a radiative diffusion cutoff wavenumber, $k_\chi = (\epsilon/\chi^3)^{1/4}$, but it ignores that aforementioned complication that on small length scales, radiation works through Newtonian heating or cooling. Finally, we have the wavenumber of the energy-carrying eddies $k_{\rm f}$, which, in the Sun, is usually being associated with the inverse pressure scale height. In our numerical experiments, on the other hand, we assume volumetric random stirring with a wavenumber comparable to the lowest wavenumber in the computational domain.

We also consider a series of experiments where large-scale heating is accomplished by imposing a uniform temperature gradient, enabling temperature fluctutions to be generated by tangling.

1.1 Governing equations

We solve the hydrodynamics equations for logarithmic density $\ln\rho$, velocity $\boldsymbol{u}$, and specific entropy s, in the form

$$\frac{{\rm D}\ln\rho}{{\rm D}t} = -\boldsymbol{\nabla}\cdot\boldsymbol{u}, \quad (1)$$

$$\rho\frac{{\rm D}\boldsymbol{u}}{{\rm D}t} = -\boldsymbol{\nabla}p + \rho\boldsymbol{f} + \boldsymbol{\nabla}\cdot(2\rho\nu\mathsf{S}), \quad (2)$$

$$\rho T\frac{{\rm D}s}{{\rm D}t} = -\boldsymbol{\nabla}\cdot\boldsymbol{F}_{\rm rad} - \beta u_z + 2\iota\rho\nu\mathsf{S}^2, \quad (3)$$

where p is the gas pressure, ν is the viscosity, $\mathsf{S} = \frac{1}{2}[\boldsymbol{\nabla}\boldsymbol{u} + (\boldsymbol{\nabla}\boldsymbol{u})^T] - \frac{1}{3}\mathsf{I}\boldsymbol{\nabla}\cdot\boldsymbol{u}$ is the traceless rate-of-strain tensor, I is the unit tensor, T is the temperature, ι and β are optional parameters ($\beta = 0$ and $\iota = 1$ is the standard case without large-scale heating and with viscous heating included), $\boldsymbol{F}_{\rm rad}$ is the radiative flux and energy supply is provided by the forcing function $\boldsymbol{f} = \boldsymbol{f}(\boldsymbol{x}, t)$, which is random in time and defined as

$$\boldsymbol{f}(\boldsymbol{x}, t) = {\rm Re}\{N\boldsymbol{f}_{\boldsymbol{k}(t)}\exp[{\rm i}\boldsymbol{k}(t)\cdot\boldsymbol{x} + {\rm i}\phi(t)]\}, \quad (4)$$

where $\boldsymbol{x}$ is the position vector. The wavevector $\boldsymbol{k}(t)$ and the random phase $-\pi < \phi(t) \le \pi$ change at every time step, so $\boldsymbol{f}(\boldsymbol{x}, t)$ is δ-correlated in time. Therefore, the normalization factor N has to be proportional to $\delta t^{-1/2}$, where δt is the length of the time step. On dimensional grounds it is chosen to

be $N = f_0 c_s(|\boldsymbol{k}|c_s/\delta t)^{1/2}$, where f_0 is a nondimensional forcing amplitude. At each timestep we select randomly one of many possible wavevectors in a certain range around a given forcing wavenumber with average value k_f. In the following, we choose $k_f/k_1 = 1.5$. The parameter ι in Equation (3) has been introduced to allow us turning off viscous heating in some of our numerical experiments.

As equation of state, we adopt a perfect gas with $p = (\mathcal{R}/\mu)T\rho$, where $\mathcal{R}$ is the universal gas constant and μ is the mean molecular weight. The pressure is related to s via $p = \rho^\gamma \exp(s/c_v)$, where the adiabatic index $\gamma = c_p/c_v$ is the ratio of specific heats at constant pressure and constant volume, respectively, and $c_p - c_v = \mathcal{R}/\mu$. To obtain the radiative flux, we adopt the gray approximation, ignore scattering, and assume that the source function S (not to be confused with the rate-of-strain tensor S) is given by the frequency-integrated Planck function, so $S = (\sigma_{SB}/\pi)T^4$, where σ_{SB} is the Stefan–Boltzmann constant. The negative divergence of the radiative flux is then given by

$$-\boldsymbol{\nabla}\cdot\boldsymbol{F}_{rad} = \kappa\rho \oint_{4\pi} (I - S)\,d\Omega, \tag{5}$$

where κ is the opacity per unit mass (assumed independent of frequency) and $I(\boldsymbol{x}, t, \hat{\boldsymbol{n}})$ is the frequency-integrated specific intensity corresponding to the energy that is carried by radiation per unit area, per unit time, in the direction $\hat{\boldsymbol{n}}$, through a solid angle $d\Omega$. We obtain $I(\boldsymbol{x}, t, \hat{\boldsymbol{n}})$ by solving the radiative transfer equation,

$$\hat{\boldsymbol{n}}\cdot\boldsymbol{\nabla} I = -\kappa\rho\,(I - S), \tag{6}$$

along a set of rays in different directions $\hat{\boldsymbol{n}}$ using the method of long characteristics. We adopt a Kramers opacity given by

$$\kappa = \kappa_0 \rho^a T^b, \tag{7}$$

where $a = 1$ and $b = -7/2$. The radiative conductivity $K(\rho, T)$ is given by

$$K(\rho, T) = \frac{16\sigma_{SB}T^3}{3\kappa\rho} = \frac{16\sigma_{SB}T^{3-b}}{3\kappa_0\rho^{a+1}}. \tag{8}$$

We are particularly interested in spectra of specific entropy, $E_s(k)$, which are normalized such that

$$\int_0^\infty E_s(k)\,dk = \tfrac{1}{2}\langle s^2\rangle. \tag{9}$$

2 Choice of parameters

We consider a cubic domain of size L^3, where $L = 1\,\mathrm{Mm}$. With our choice of $k_f/k_1 = 1.5$, this implies $k_f \approx 10\,\mathrm{Mm}^{-1}$. We use 576^3 meshpoints. For the viscosity we choose $\nu = 10^{-3}\,\mathrm{Mm\,km\,s^{-1}}$. We choose $f_0 = 0.1$, which results in an rms velocity of about $4\,\mathrm{km\,s^{-1}}$. The Reynolds number is then

$$\mathrm{Re} = u_{rms}/\nu k_f = 420. \tag{10}$$

The initial density is $\rho = 4\times10^{-4}\,\mathrm{g\,cm^{-3}}$, $T = 36,000\,\mathrm{K}$ (initially $39,000\,\mathrm{K}$, but can cool down to $34,000\,\mathrm{K}$), $c_s = 30\,\mathrm{km\,s^{-1}}$, $p = 0.2\,\mathrm{g\,cm^{-3}\,km^2\,s^{-2}}$. For the radiation transport, we use 6 rays. This turns out to be sufficient, because a comparison with 14 and 22 rays did not result in noticeable differences,

3 Cooling times

To provide background for the interpretation of our results, we discuss first the dependence of the radiative cooling rate λ on the mean-free path and the wavenumber k of the temperatures structures. It is given by (see Appendix A of Barekat & Brandenburg, 2014, for details)

$$\lambda = \frac{c_\gamma \ell k^2/3}{1+\ell^2k^2/3} = \begin{cases} c_\gamma \ell k^2/3 \\ c_\gamma/\ell \end{cases} \tag{11}$$

Optically thick if $\ell^2k^2/3 \ll 1$.

$$\lambda = (c_\gamma/\ell)\,\min(1, \ell^2k^2/3). \tag{12}$$

See Table 1.

4 Advection tests

Advection tends to sharpen the temperature jump, while radiation tends to smoothen it. Thus, we expect that with decreasing for opacity and thus increasing mean-free path, the thermal diffusivity, given by $\chi = c_\gamma\ell/3$, the temperature profile should become smoother. However, when the opacity decreases further, the mean-free path begins to exceed the viscous length scale, $\sim \nu/U_0$, where U_0 is the magnitude of the advection velocity. When that is the case, the medium becomes essentially optically thin on those small length scales, and radiation thus loses its diffusing properties. We thus expect ...

5 Results

Figure ?? shows the results of a numerical experiment using a sinusoidal initial condition for the specific entropy.

We expect *insulation* and inefficient cooling at wavenumbers above $\kappa\rho$. This is not obvious from the numerical results which show that the spectral

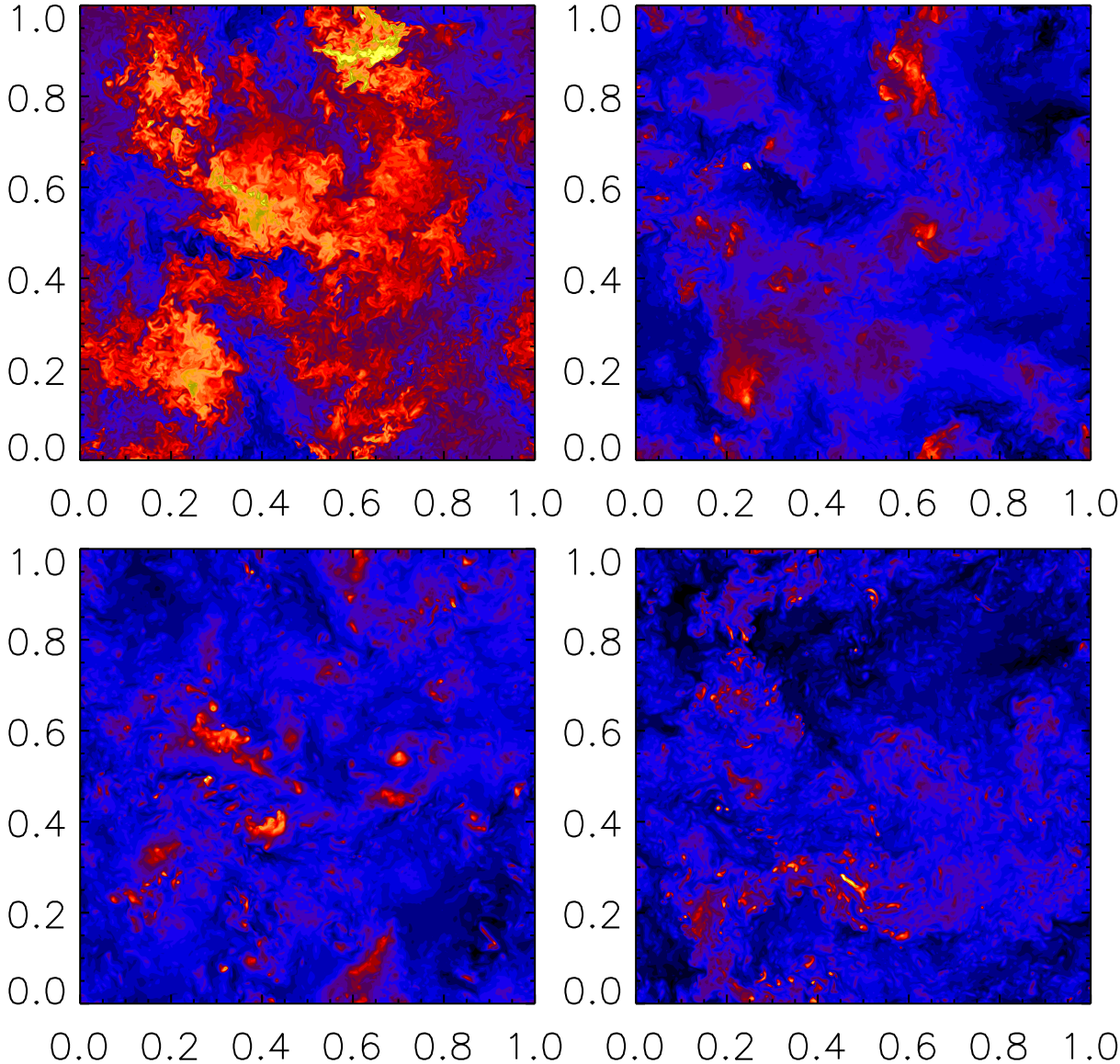

Figure 5: Images for 4, 40, 400, and 4000. add x [Mm]

Table 2: Parameters.

Series	A	B	C
visc heat	yes	yes	no
β	0	5×10^{-3}	
$u_{\rm rms}$	3.5	3.8	
Re	1800	400	
$\epsilon_{\rm K}$	....	....	

specific entropy is actually independent of the opacity. Furthermore, the spectral specific entropy increases with wavenumber, which is opposite to the behavior spectral kinetic energy. This is clearly a consequence of the somewhat unusual source of heating which is viscous heating and therefore naturally a small-scale phenomenon.

Discuss instability of descending blobs. Visualize them. Do decay simulation.

References

Barekat, A., & Brandenburg, A. 2014, A&A, 571, A68

Spruit, H. C. 1974, Solar Phys., 34, 277

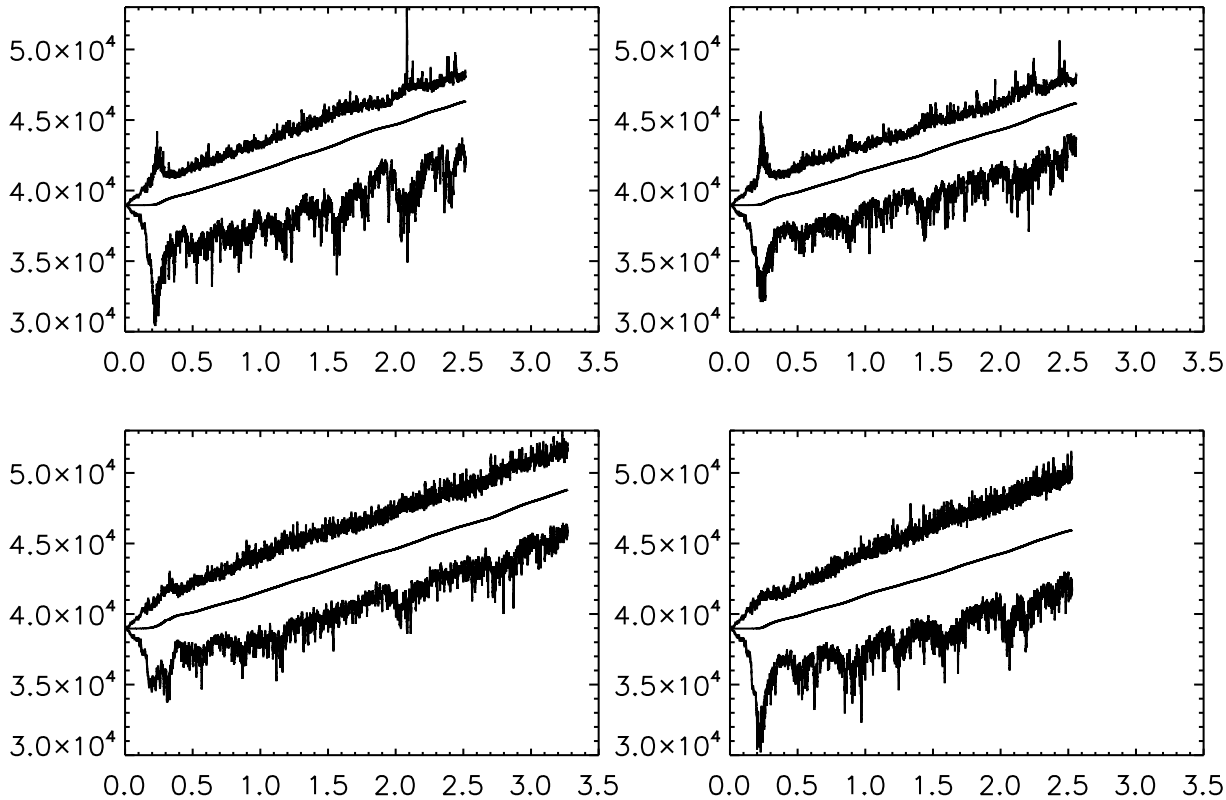

Figure 6: Temperature evolution for 4, 40, 400, and 4000.

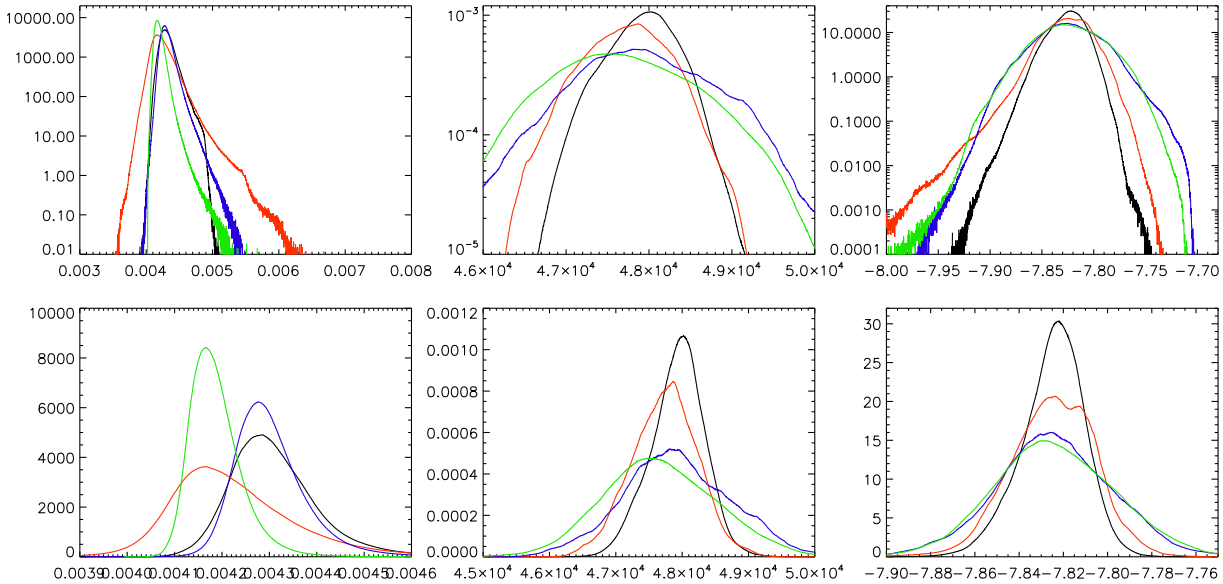

Figure 7: PDFs for 4, 40, 400, and 4000.

$Header: /var/cvs/brandenb/tex/notes/photo/notes.tex,v 1.22 2019/04/15 10:29:35 brandenb Exp $

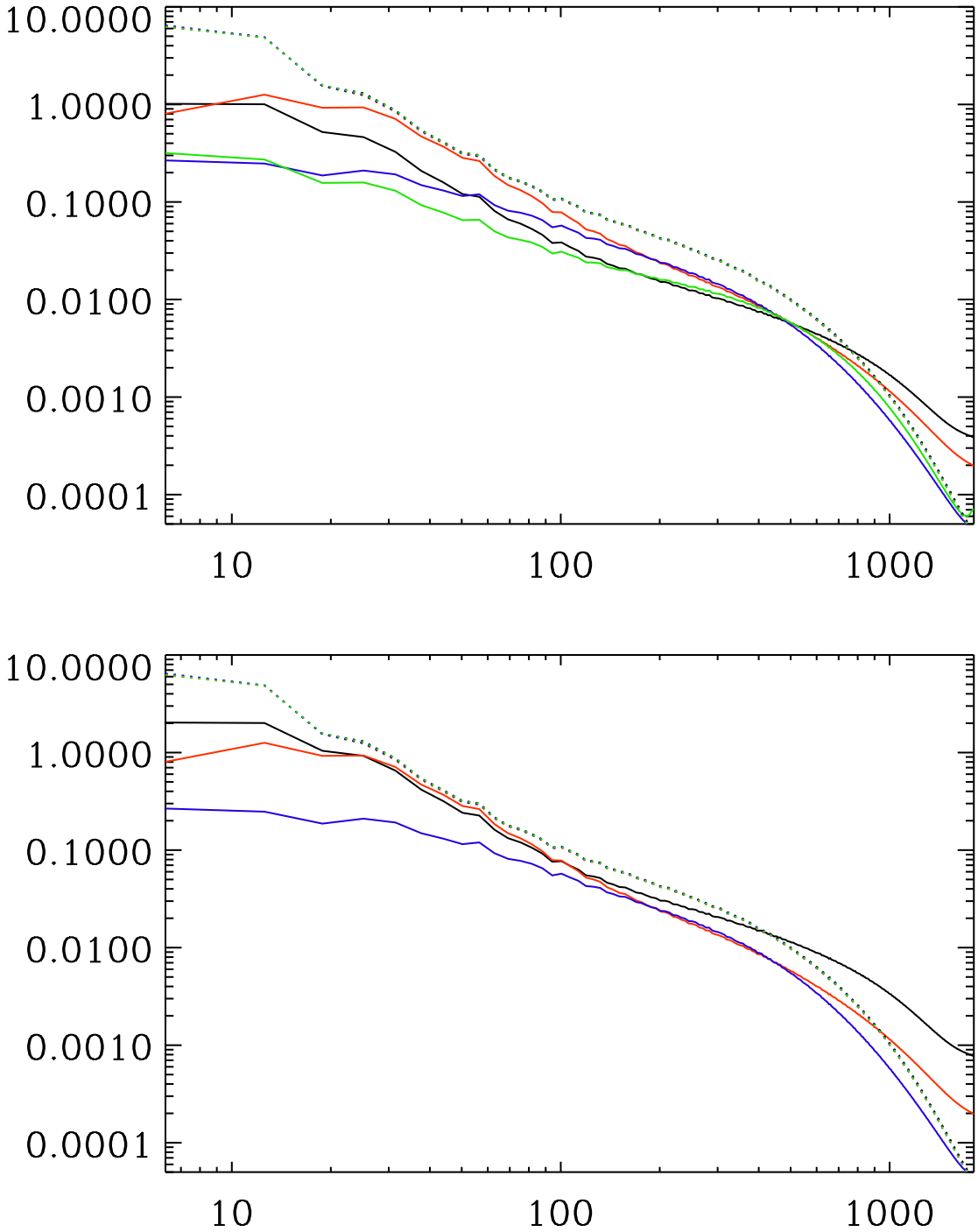

Figure 8: Spectra `pspec_comp576` and `pspec_comp576b`.

Table 1: Cooling times based on $c_\gamma = 3\,\mathrm{km\,s^{-1}}$, which is relevant for $\rho = 4\times10^{-4}\,\mathrm{g\,cm^{-3}}$ and $T = 36,000\,\mathrm{K}$. Here, $\mathrm{Pe} = u_{\mathrm{rms}}/\chi k_{\mathrm{f}}$.

Pr	ℓ $k_\gamma = \kappa\rho$	λ $c_\gamma k_\gamma$	τ $(c_\gamma k_\gamma)^{-1}$	χ $c_\gamma/3k_\gamma$	Pe
0.004	$4\,\mathrm{Mm^{-1}}$	$12\,\mathrm{ks^{-1}}$	$0.1\,\mathrm{ks}$	0.25	1.6
0.04	$40\,\mathrm{Mm^{-1}}$	$120\,\mathrm{ks^{-1}}$	$0.01\,\mathrm{ks}$	0.025	16
0.4	$400\,\mathrm{Mm^{-1}}$	$1200\,\mathrm{ks^{-1}}$	$0.001\,\mathrm{ks}$	0.0025	160
4	$4000\,\mathrm{Mm^{-1}}$	$12000\,\mathrm{ks^{-1}}$	$0.0001\,\mathrm{ks}$	0.00025	1600

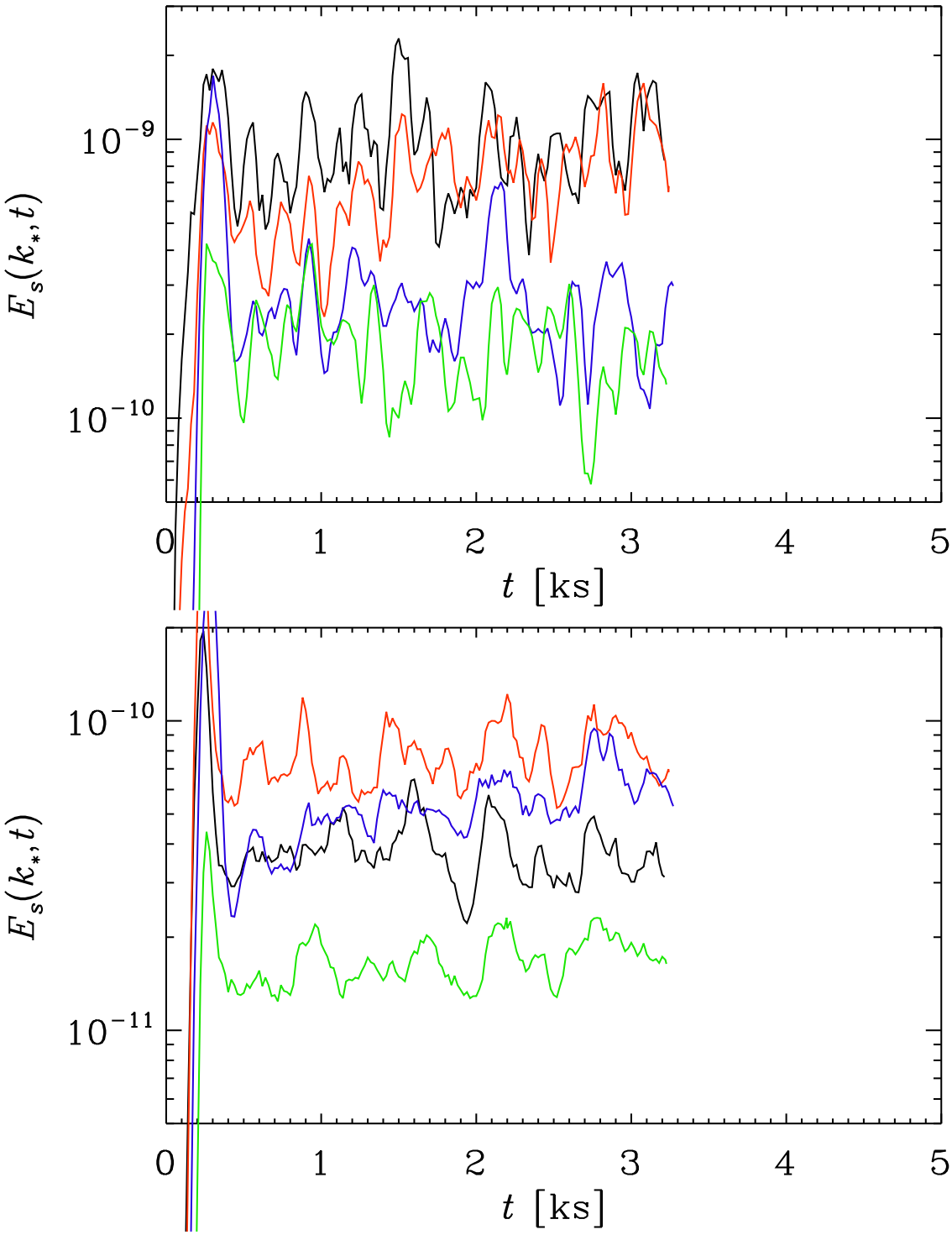

Figure 9: Temporal evolution at $k = 6$ (top) and 100 (bottom)

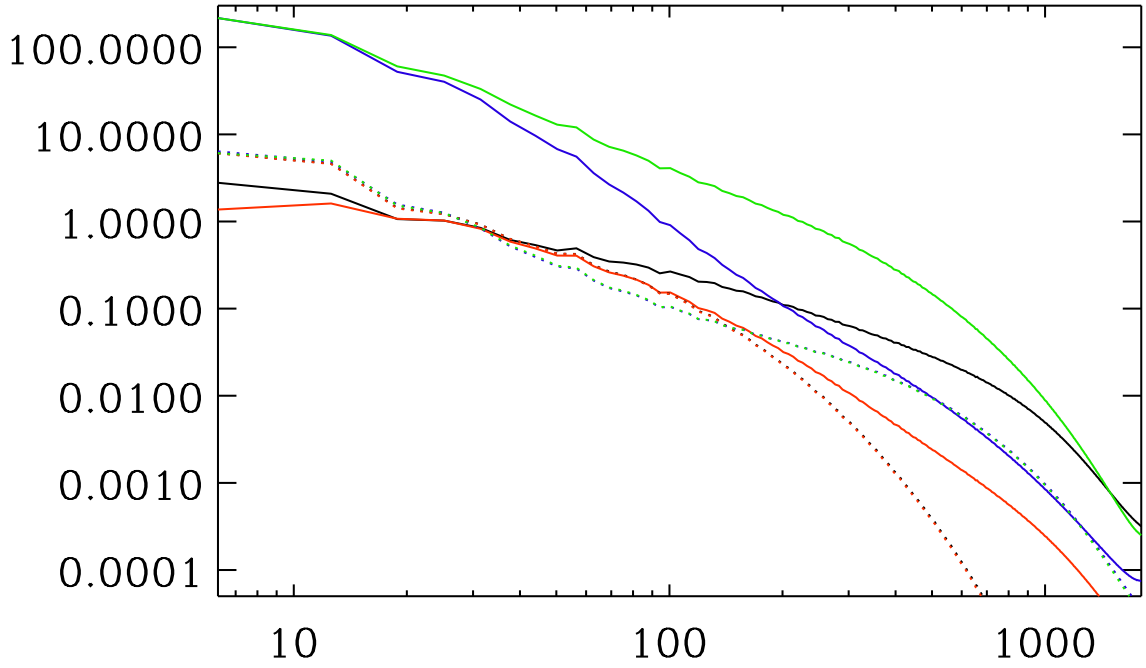

Figure 10: Spectra `pspec_comp576a_grad_novheat`

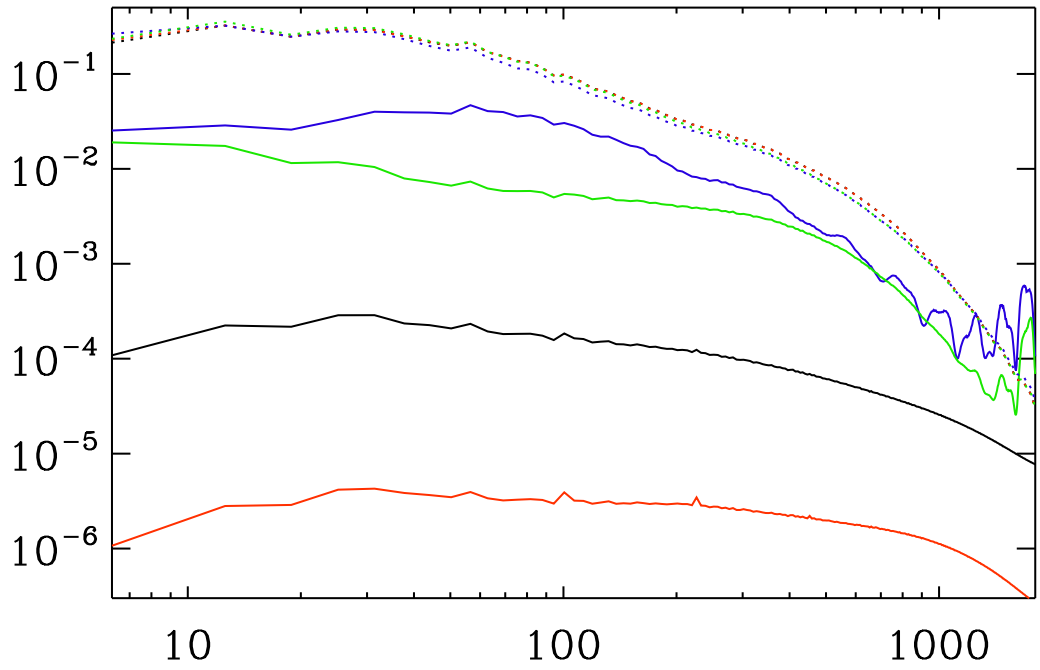

Figure 11: Spectra in the optically thin cases with $k_\gamma = 40$ (black) and 400 (red) and the optically thick cases with $k_\gamma = 40$ (blue) and 400 (green).